J. Nonlinear Funct. Anal. 2026 (2026) 6 https://doi.org/10.23952/jnfa.2026.6

MATHRES
Journal of Nonlinear Functional Analysis
Available online at http://jnfa.mathres.org

A NEW UNCONDITIONALLY ENERGY-STABLE FINITE DIFFERENCE SCHEME FOR RIESZ SPACE-FRACTIONAL ALLEN-CAHN EQUATIONS

HAIFENG SANG, TIANLIANG HOU*

School of Mathematics and Statistics, Beihua University, Jilin 132013, China

Abstract. In this paper, we present a new second-order finite difference scheme for Riesz space-fractional Allen-Cahn equations. We use a modified Crank-Nicolson finite difference scheme with stabilized terms of third-order numerical accuracy for temporal discretization. The discrete maximum bound principle, the maximum-norm error estimates, and the discrete energy stability of the proposed scheme are discussed. It is demonstrated that the proposed scheme is maximum bound principle preserving and unconditionally energy-stable for any nonnegative stabilization parameter β which satisfies $0 \leq \beta \leq 1/4$. As far as we know, the proposed fully implicit second-order scheme has never been proved to preserve the maximum bound principle before except the Allen-Cahn equation with $\beta = 1/12$ and $\beta = 0$. Finally, some numerical experiments are performed to verify the theoretical results.

Keywords. Riesz space-fractional Allen-Cahn equation; Error estimate; Energy stability; Finite difference method; Maximum bound principle.

2020 MSC. 65M06, 65M15, 41A05.

1. Introduction

In this paper, we consider the finite difference approximation for the following 1D space-fractional Allen-Cahn equation

$$\frac{\partial u(x,t)}{\partial t} = \varepsilon^2 \frac{\partial^\alpha u(x,t)}{\partial |x|^\alpha} - f(u),\ x \in (a,b), t \in (0,T], \tag{1.1}$$

$$u(x,0) = u_0(x),\ x \in [a,b], \tag{1.2}$$

$$u(a,t) = u(b,t) = 0,\ t \in (0,T]. \tag{1.3}$$

*Corresponding author.
E-mail address: 270854140@qq.com (T. Hou).
Received August 27, 2025; Accepted January 8, 2026.

Here the parameter $\varepsilon > 0$, $\alpha \in (1,2)$, the nonlinear term $f(u) = u^3 - u$ presents the polynomial double well potential, $\frac{\partial^\alpha}{\partial |x|^\alpha}$ denotes the Riesz fractional derivative operator, which is defined by

$$\frac{\partial^\alpha u(x,t)}{\partial |x|^\alpha} = -\frac{1}{2\cos\frac{\alpha\pi}{2}\Gamma(2-\alpha)}\frac{\mathrm{d}^2}{\mathrm{d}x^2}\int_{-\infty}^{\infty} |x-\xi|^{1-\alpha} u(\xi,t)\,\mathrm{d}\xi,$$

where

$$\Gamma(z) = \int_0^\infty t^{z-1}e^{-t}\mathrm{d}t, z > 0.$$

In recent years, there has been significant interest in using the diffusive-interface phase-field approach for modeling the mesoscale morphological pattern formation and interface motion. One of the very effective mathematical models describing these physical phenomena is the Allen-Cahn equation introduced in 1979 [1]. Similar to the classical Allen-Cahn equation, the space-fractional Allen-Cahn equation (1.1)-(1.3) also has the following two intrinsic properties. One is the maximum bound principle, i.e., if $|u_0(x)| \leq 1$ for all $x \in [a,b]$, then $|u(x,t)| \leq 1$ for all $x \in [a,b]$ and $t \geq 0$. The other is the energy function $E(u)$ is decreasing with time: $E(u(t_n)) \leq E(u(t_m))$, $\forall t_n > t_m$, where $E(u) = \int_a^b \left(F(u) - \frac{1}{2}\varepsilon^2 u \frac{\partial^\alpha u}{\partial |x|^\alpha}\right)\mathrm{d}x$ and $F(u) = \frac{1}{4}(u^2-1)^2$. Such two properties are important in the study of the stability of the solution to the Allen-Cahn equation, and whether they could be inherited in the discrete level is a significant issue in numerical simulations. Tang and Yang [11] discussed the discrete maximum bound principle and the discrete energy stability of first-order linear implicit-explicit scheme for the Allen-Cahn equation. Shen et al. [10] analyzed the discrete maximum bound principle of first-order linear implicit-explicit scheme for the generalized Allen-Cahn equation. For temporal discretization, the standard semi-implicit scheme as well as the stabilized semi-implicit scheme were adopted, while for space discretization, the central finite difference was used for approximating the diffusion term and the upwind scheme was employed for the advection term. Hou et al. [4] considered the discrete maximum bound principle, the discrete energy stability and the error estimates of the second-order Crank-Nicolson finite difference scheme for fractional-in-space Allen-Cahn equations with Riemann-Liouville fractional derivatives. Liao et al. [7] presented a second-order and nonuniform time-stepping maximum bound principle preserving scheme for time-fractional Allen-Cahn equations. Du et al. [2] proposed the first-order and the second-order maximum bound principle preserving exponential time differencing schemes for the nonlocal Allen-Cahn equation. To obtain a higher-order scheme for solving the Allen-Cahn equation, Li et al. [9] proposed a new class of maximum principle preserving numerical schemes, which consists of a k_{th}-order multistep exponential integrator in time, and a lumped mass finite-element method in space with piecewise r_{th}-order polynomials and Gauss-Lobatto quadrature. Zhang et al. [16] proposed high-order (up to fourth) strong stability-preserving implicit-explicit Runge-Kutta schemes for the time integration of the space-fractional Allen-Cahn equation and discussed the discrete maximum bound principle and energy stability. Ju et al. [6] developed and analyzed novel first- and second-order linear numerical schemes for a class of Allen-Cahn type gradient flows. These schemes combined the generalized scalar auxiliary variable approach and the exponential time integrator with a stabilization term, while the standard central difference stencil was used for discretization of the spatial differential operator. The authors not only proved their unconditional preservation of the energy dissipation law and the maximum bound principle in the discrete setting, but also derived their optimal temporal error estimates under fixed spatial mesh. Weng et al. [12] considered a nonlocal ternary conservative Allen-Cahn model, where the standard Laplace operator was intentionally replaced with a spatial convolution term that aims at describing long-range interactions among particles. They developed a linear energy stable scheme based on the operator splitting method and discussed the mass conservation, energy stability and global convergence of the new scheme. Zhai et al. [15] presented a new energy dissipation and maximum bound principle preserving scheme based on the operator splitting method for solving a nonlocal ternary Allen-Cahn model. The discrete maximum bound principle and global convergence of the new scheme were analyzed rigorously. This is the first work to show that the operator splitting method can guarantee the maximum bound principle for a ternary Allen-Cahn model. Xu et al. [14] presented an unconditionally energy-stable finite difference scheme for Riesz space-fractional Allen-Cahn equations. A stabilizing term $\mathscr{O}(\tau(U^{n+1}-U^{n+1}))$ was added to the proposed scheme to maintain numerical stability.

In this work, we present an unconditionally energy-stable second-order finite difference scheme for the Allen-Cahn equation with Riesz fractional derivative. We can prove that our scheme is maximum bound principle preserving and the discrete energy is unconditionally decreasing when the stabilization parameter satisfies $0 \le \beta \le 1/4$. As far as we know, the proposed fully implicit second-order scheme has never been proved to preserve the maximum bound principle before except Allen-Cahn equation [5] with $\beta = 1/12$, time-fractional Allen-Cahn equation [8] with $\beta = 1/12$, Riesz space-fractional Allen-Cahn equation [14] with $\beta = 1/12$ and Riesz space-fractional Allen-Cahn equation [13] with $\beta = 0$. The proof techniques used in the proof of discrete maximum bound principle are different from those used in References [5, 8, 13, 14].

The rest of the paper is organized as follows. In Section 2, a stabilized second-order finite difference scheme will be presented. The discrete maximum bound principle, the maximum-norm error estimate and the discrete energy stability of the proposed scheme will be discussed in Sections 3-4, respectively. Finally, some numerical examples are given in the last section to verify the theoretical results.

2. Finite Difference Approximation

We partition the interval (a,b) into a uniform mesh with the space step $h = (b-a)/(N+1)$ and $\tau = T/M$, where N and M are two positive integers. The set of grid points is denoted by $x_i = a + (i-1)h$ and $t_n = n\tau$ for $1 \le i \le N+2$ and $0 \le n \le M$. We use the notations $u^n = u(x,t_n)$ and $u_i^n = u(x_i,t_n)$. Define $V_h = \left\{v : v = \{v_i\} \text{ is a grid function in } \{x_i = a + ih\}_{i=1}^{N}\right\}$. For any $v = \{v_i\} \in V_h$, we define its pointwise maximum norm $\|v\|_\infty = \max_{1\le i\le N} |v_i|$. We adopt a second order finite difference approach in [3] to discretize the fractional operator $\frac{\partial^\alpha}{\partial |x|^\alpha}$. Hereinafter, we denote D_h as the discretization matrix of the fractional operator. It is given by

$$D_h = -\frac{1}{h^\alpha}\begin{bmatrix} g_0 & g_{-1} & g_{-2} & \cdots & g_{-N+1} \\ g_1 & g_0 & g_{-1} & \ddots & g_{-N+2} \\ g_2 & g_1 & g_0 & \ddots & g_{-N+3} \\ \vdots & \vdots & \vdots & \ddots & \vdots \\ g_{N-1} & g_{N-2} & g_{N-3} & \cdots & g_0 \end{bmatrix}_{N\times N} =: -\frac{1}{h^\alpha}A, \tag{2.1}$$

where

$$g_0 = \frac{\Gamma(\alpha+1)}{\Gamma\left(\frac{\alpha}{2}+1\right)^2} > 0,\ g_{-k} = g_k < 0,\ \sum_{k=-\infty}^{+\infty} g_k = 0, \tag{2.2}$$

and

$$g_{k+1} = \left(1 - \frac{\alpha+1}{\frac{\alpha}{2}+k+1}\right) g_k < 0, 1 < \alpha < 2. \tag{2.3}$$

By use of (2.1)-(2.3), it is sufficient to prove that D_h satisfies the following properties. Here we omit the proof.

Lemma 2.1. *The matrix D_h satisfies the following properties:*

- *D_h is symmetric;*
- *D_h is negative definite, i.e., $U^T D_h U < 0$, for any nonzero $U \in \mathbf{R}^N$;*
- *The elements of $D_h = (b_{ij})$ satisfy*

$$b_{ii} = -d < 0,\ d \geq \max_i \sum_{j \neq i} |b_{ij}|. \tag{2.4}$$

Next, we present the following modified Crank-Nicolson finite difference scheme with stabilized term to solve equation (1.1), namely,

$$\begin{aligned} \frac{U^{n+1}-U^n}{\tau} &+ \frac{\left(U^{n+1}\right)^{.3} + \left(U^{n+1}\right)^{.2} U^n + U^{n+1}\left(U^n\right)^{.2} + \left(U^n\right)^{.3}}{4} \\ &- \frac{U^{n+1}+U^n}{2} + \beta\left(U^{n+1}-U^n\right)^{.3} = \frac{\varepsilon^2 D_h \left(U^{n+1}+U^n\right)}{2}, \end{aligned} \tag{2.5}$$

where $0 \leq n \leq M-1$, $0 \leq \beta \leq \frac{1}{4}$, and U^n represents the vector of numerical solution at nth level. Hereinafter we define

$$U^n := (U_1^n, U_2^n, \cdots, U_N^n)^T,$$

$$(U^n)^{.2} := ((U_1^n)^2, (U_2^n)^2, \cdots, (U_N^n)^2)^T,$$

$$(U^n)^{.3} := ((U_1^n)^3, (U_2^n)^3, \cdots, (U_N^n)^3)^T,$$

and

$$U^n V^n := (U_1^n V_1^n, U_2^n V_2^n, \cdots, U_N^n V_N^n)^T.$$

3. The Discrete Maximum Bound Principle

In this section, we discuss the discrete maximum bound principle for scheme (2.5). We find that the following result not only simplifies the proof when the stabilization parameter $\beta = 0$ [13] but also extends the results of $\beta = 0$ [13] and $\beta = \frac{1}{12}$ [5, 8, 14] to $0 \leq \beta \leq \frac{1}{4}$.

Theorem 3.1. *Assume that the initial value satisfies $\max_{x\in[a,b]} |u_0(x)| \leq 1$. Then the fully discrete scheme (2.5) preserves the discrete maximum bound principle provided that the time step size* *satisfies*

$$\tau \le \min\left\{\frac{1}{4}, \frac{h^{\alpha}\Gamma\left(\frac{\alpha}{2}+1\right)^2}{\varepsilon^2\Gamma(\alpha+1)}\right\},\ \beta=\frac{1}{4};$$

$$\tau \le \min\left\{\frac{1}{2(1+12\beta)}, \frac{h^{\alpha}\Gamma\left(\frac{\alpha}{2}+1\right)^2}{\varepsilon^2\Gamma(\alpha+1)}\right\},\ 0\le\beta<\frac{1}{4}.$$

Proof. We prove this theorem by induction. First, it follows from the assumption on $u_0(x)$ that $||U^0||_\infty \le 1$. We now assume that the result holds for $n=m$ i.e., $||U^m||_\infty \le 1$. Below, we check that this upper bound is also true for $n=m+1$. If $\|U^{m+1}\|_\infty = |U_p^{m+1}|$, then $|U_p^{m+1}| \ge |U_j^{m+1}|$ for all $1\le j\le N$. Next, we divide the proof into three cases:
Case I: $\beta=\frac{1}{4}$.

We rewrite (2.5) as

$$\left(1-\frac{\tau}{2}\right)U^{m+1}+\frac{\tau}{2}\left(U^{m+1}\right)^{.3}+\tau U^{m+1}\left(U^m\right)^{.2}-\frac{\tau}{2}\varepsilon^2 D_h U^{m+1} = \left(1+\frac{\tau}{2}\right)U^m+\frac{\tau}{2}U^m\left(U^{m+1}\right)^{.2}+\frac{\tau}{2}\varepsilon^2 D_h U^m. \tag{3.1}$$

The p-th component of (3.1) is

$$\left[1-\frac{\tau}{2}+\tau\left(U_p^m\right)^2\right]U_p^{m+1}+\frac{\tau}{2}\left(U_p^{m+1}\right)^3-\frac{\tau}{2}\varepsilon^2\sum_{j=1}^N b_{pj}U_j^{m+1} = \frac{1}{2}U_p^m+\frac{\tau}{2}\varepsilon^2\sum_{j=1}^N b_{pj}U_j^m+\frac{1+\tau}{2}U_p^m+\frac{\tau}{2}U_p^m\left(U_p^{m+1}\right)^2. \tag{3.2}$$

By $\tau\le\frac{1}{4}$ and (2.4), we find that $\left[1-\frac{\tau}{2}+\tau\left(U_p^m\right)^2\right]U_p^{m+1}$, $\frac{\tau}{2}\left(U_p^{m+1}\right)^3$ and $-\frac{\tau}{2}\varepsilon^2\sum_{j=1}^N b_{pj}U_j^{m+1}$ are nonpositive or nonnegative simultaneously. Then, we have

$$\begin{aligned}
&\left|\left[1-\frac{\tau}{2}+\tau\left(U_p^m\right)^2\right]U_p^{m+1}+\frac{\tau}{2}\left(U_p^{m+1}\right)^3-\frac{\tau}{2}\varepsilon^2\sum_{j=1}^N b_{pj}U_j^{m+1}\right| \\
=&\left|\left[1-\frac{\tau}{2}+\tau\left(U_p^m\right)^2\right]U_p^{m+1}\right|+\left|\frac{\tau}{2}\left(U_p^{m+1}\right)^3\right|+\left|\frac{\tau}{2}\varepsilon^2\sum_{j=1}^N b_{pj}U_j^{m+1}\right| \\
\ge&\left[1-\frac{\tau}{2}+\tau\left(U_p^m\right)^2\right]\left|U_p^{m+1}\right|+\frac{\tau}{2}\left|U_p^{m+1}\right|^3.
\end{aligned} \tag{3.3}$$

Taking the absolute value of (3.2), using (3.3), $\tau\le\frac{h^{\alpha}\Gamma\left(\frac{\alpha}{2}+1\right)^2}{\varepsilon^2\Gamma(\alpha+1)}$, (2.4) and $\|U^m\|_\infty\le 1$, we easily obtain

$$\begin{aligned}
&\left(1-\frac{\tau}{2}\right)\left|U_p^{m+1}\right|+\tau\left(U_p^m\right)^2\left|U_p^{m+1}\right|+\frac{\tau}{2}\left|U_p^{m+1}\right|^3 \\
\le&\left|\frac{1}{2}U_p^m+\frac{\tau}{2}\varepsilon^2\sum_{j=1}^N b_{pj}U_j^m\right|+\frac{1+\tau}{2}\left|U_p^m\right|+\left|\frac{\tau}{2}U_p^m\left(U_p^{m+1}\right)^2\right| \\
\le&\frac{1}{2}+\frac{1}{2}\left|U_p^m\right|+\frac{\tau}{2}+\frac{\tau}{2}\left|U_p^{m+1}\right|^2,
\end{aligned} \tag{3.4}$$

where we used

$$
\begin{aligned}
\left|\frac{1}{2}U_p^m+\frac{\tau}{2}\varepsilon^2\sum_{j=1}^N b_{pj}U_j^m\right| &= \left|\left(\frac{1}{2}+\frac{\tau}{2}\varepsilon^2 b_{pp}\right)U_p^m+\frac{\tau}{2}\varepsilon^2\sum_{j\neq p} b_{pj}U_j^m\right| \\
&\leq \left(\frac{1}{2}+\frac{\tau}{2}\varepsilon^2 b_{pp}\right)\left|U_p^m\right|+\frac{\tau}{2}\varepsilon^2\sum_{j\neq p}\left|b_{pj}\right|\left|U_j^m\right| \\
&\leq \frac{1}{2}+\frac{\tau}{2}\varepsilon^2 b_{pp}+\frac{\tau}{2}\varepsilon^2\sum_{j\neq p}\left|b_{pj}\right| \\
&= \frac{1}{2}+\frac{\tau}{2}\varepsilon^2\left(\sum_{j\neq p}\left|b_{pj}\right|-d\right) \\
&\leq \frac{1}{2}.
\end{aligned} \tag{3.5}
$$

It follows from (3.4) that

$$\left(1-\frac{\tau}{2}\right)\left|U_p^{m+1}\right|+\tau\left|U_p^m\right|^2\left|U_p^{m+1}\right|+\frac{\tau}{2}\left(\left|U_p^{m+1}\right|-1\right)\left|U_p^{m+1}\right|^2\leq\frac{1}{2}+\frac{\tau}{2}+\frac{1}{2}\left|U_p^m\right|. \tag{3.6}$$

If $\left\|U^{m+1}\right\|_\infty>1$, then (3.6) becomes $1-\frac{\tau}{2}+\tau\left|U_p^m\right|^2<\frac{1}{2}+\frac{\tau}{2}+\frac{1}{2}\left|U_p^m\right|$, namely,

$$-\tau\left|U_p^m\right|^2+\frac{1}{2}\left|U_p^m\right|+\tau-\frac{1}{2}>0,$$

which contradicts $\left|U_p^m\right|\leq\|U^m\|_\infty\leq 1$ provided that $\tau\leq\frac{1}{4}$. Then the bound $\left\|U^{m+1}\right\|_\infty\leq 1$ holds.

Case II: $\frac{1}{12}\leq\beta<\frac{1}{4}$.

We rewrite (2.5) as

$$
\begin{aligned}
&\left(1-\frac{\tau}{2}\right)U^{m+1}+\left(\frac{1}{4}+\beta\right)\tau\left(U^{m+1}\right)^{.3}+\left(\frac{1}{4}+3\beta\right)\tau U^{m+1}\left(U^m\right)^{.2}-\frac{\tau}{2}\varepsilon^2 D_h U^{m+1} \\
&\quad=\left(1+\frac{\tau}{2}\right)U^m+\left(3\beta-\frac{1}{4}\right)\tau U^m\left(U^{m+1}\right)^{.2}+\frac{\tau}{2}\varepsilon^2 D_h U^m+\left(\beta-\frac{1}{4}\right)\tau\left(U^m\right)^{.3}.
\end{aligned} \tag{3.7}
$$

The p-th component of (3.7) is

$$
\begin{aligned}
&\left(1-\frac{\tau}{2}\right)U_p^{m+1}+\left(\frac{1}{4}+3\beta\right)\tau\left(U_p^m\right)^2U_p^{m+1}+\left(\frac{1}{4}+\beta\right)\tau\left(U_p^{m+1}\right)^3-\frac{\tau}{2}\varepsilon^2\sum_{j=1}^N b_{pj}U_j^{m+1} \\
&=\left(1+\frac{\tau}{2}\right)U_p^m+\frac{\tau}{2}\varepsilon^2\sum_{j=1}^N b_{pj}U_j^m+\left(3\beta-\frac{1}{4}\right)\tau U_p^m\left(U_p^{m+1}\right)^2+\left(\beta-\frac{1}{4}\right)\tau\left(U_p^m\right)^3 \\
&=\underbrace{\frac{1}{2}U_p^m+\frac{\tau}{2}\varepsilon^2\sum_{j=1}^N b_{pj}U_j^m}+\left(3\beta-\frac{1}{4}\right)\tau U_p^m\left(U_p^{m+1}\right)^2+\frac{1}{4}U_p^m+\left(\beta+\frac{1}{4}\right)\tau U_p^m \\
&\quad\underbrace{+\frac{1}{4}U_p^m+\left(\frac{1}{4}-\beta\right)\tau U_p^m-\left(\frac{1}{4}-\beta\right)\tau\left(U_p^m\right)^3}.
\end{aligned} \tag{3.8}
$$

Let

$$g(x)=\frac{1}{4}x+\left(\frac{1}{4}-\beta\right)\tau x-\left(\frac{1}{4}-\beta\right)\tau x^3, x\in[-1,1].$$

It is easy to see that $g'(x)=\frac{1}{4}+\left(\frac{1}{4}-\beta\right)\tau-\left(\frac{3}{4}-3\beta\right)\tau x^2$ and $g'(x)\geq 0$ for $\tau\leq\frac{1}{2-8\beta}$. By $g(1)=-g(-1)=\frac{1}{4}$, we have $|g(x)|\leq\frac{1}{4}$, so

$$\left|\frac{1}{4}U_p^m+\left(\frac{1}{4}-\beta\right)\tau U_p^m-\left(\frac{1}{4}-\beta\right)\tau\left(U_p^m\right)^3\right|\leq\frac{1}{4}. \tag{3.9}$$

Taking the absolute value of (3.8) and using (3.5), (3.9) and $\|U^m\|_\infty\leq 1$, we easily obtain

$$\begin{aligned}\left(1-\frac{\tau}{2}\right)\left|U_p^{m+1}\right|+\left(\frac{1}{4}+3\beta\right)\tau\left(U_p^m\right)^2\left|U_p^{m+1}\right|+\left(\frac{1}{4}+\beta\right)\tau\left|U_p^{m+1}\right|^3\\ \leq\frac{1}{2}+\left(3\beta-\frac{1}{4}\right)\tau\left|U_p^{m+1}\right|^2+\frac{1}{4}\left|U_p^m\right|+\beta\tau+\frac{\tau}{4}+\frac{1}{4}.\end{aligned}$$

If $\left\|U^{m+1}\right\|_\infty>1$, we find that

$$\begin{aligned}\left(1-\frac{\tau}{2}\right)+\left(\frac{1}{4}+3\beta\right)\tau\left|U_p^m\right|^2+\left(\frac{1}{4}+\beta\right)\tau\left|U_p^{m+1}\right|^3\\ <\frac{3}{4}+\left(3\beta-\frac{1}{4}\right)\tau\left|U_p^{m+1}\right|^3+\frac{1}{4}\left|U_p^m\right|+\beta\tau+\frac{\tau}{4}.\end{aligned}$$

namely,

$$\left(1-\frac{\tau}{2}\right)+\left(\frac{1}{4}+3\beta\right)\tau\left|U_p^m\right|^2+\left(\frac{1}{2}-2\beta\right)\tau\left|U_p^{m+1}\right|^3<\frac{3}{4}+\frac{1}{4}\left|U_p^m\right|+\beta\tau+\frac{\tau}{4}.$$

Using the assumption $\left\|U^{m+1}\right\|_\infty>1$ again, we get

$$-\left(\frac{1}{4}+3\beta\right)\tau\left|U_p^m\right|^2+\frac{1}{4}\left|U_p^m\right|+\left(\frac{1}{4}+3\beta\right)\tau-\frac{\tau}{4}>0,$$

which is in contradiction with $\left|U_p^m\right|\leq\|U^m\|_\infty\leq 1$ provided that $\tau\leq\frac{1}{2(1+12\beta)}$. It is obvious that $\left\|U^{m+1}\right\|_\infty\leq 1$.

Case III: $0\leq\beta<\frac{1}{12}$.

Now, we rewrite (3.8) as

$$\begin{aligned}&\left(1-\frac{\tau}{2}\right)U_p^{m+1}+\left(\frac{1}{4}+3\beta\right)\tau\left(U_p^m\right)^2U_p^{m+1}+\left(\frac{1}{4}+\beta\right)\tau\left(U_p^{m+1}\right)^3-\frac{\tau}{2}\varepsilon^2\sum_{j=1}^N b_{pj}U_j^{m+1}\\ =&\underbrace{\frac{1}{2}U_p^m+\frac{\tau}{2}\varepsilon^2\sum_{j=1}^N b_{pj}U_j^m}+\left(3\beta-\frac{1}{4}\right)\tau U_p^m\left[\left(U_p^{m+1}\right)^2-1\right]+\frac{1}{4}U_p^m+4\beta\tau U_p^m\\ &+\underbrace{\frac{1}{4}U_p^m+\left(\frac{1}{4}-\beta\right)\tau U_p^m-\left(\frac{1}{4}-\beta\right)\tau\left(U_p^m\right)^3}.\end{aligned} \tag{3.10}$$

Taking the absolute value of (3.10), then using (3.5), (2.4) and $\|U^m\|_\infty \le 1$, we conclude that

$$\left(1-\frac{\tau}{2}\right)\left|U_p^{m+1}\right| + \left(\frac{1}{4}+3\beta\right)\tau\left(U_p^m\right)^2\left|U_p^{m+1}\right| + \left(\frac{1}{4}+\beta\right)\tau\left|U_p^{m+1}\right|^3$$
$$\le \frac{1}{2} + \left(\frac{1}{4}-3\beta\right)\tau\left|\left(U_p^{m+1}\right)^2-1\right| + \frac{1}{4}\left|U_p^m\right| + 4\beta\tau + \frac{1}{4}.$$

Suppose $\left\|U^{m+1}\right\|_\infty > 1$. Then

$$\left(1-\frac{\tau}{2}\right) + \left(\frac{1}{4}+3\beta\right)\tau\left(U_p^m\right)^2 + \left(\frac{1}{4}+\beta\right)\tau\left|U_p^{m+1}\right|^3$$
$$< \frac{3}{4} + \left(\frac{1}{4}-3\beta\right)\tau\left[\left(U_p^{m+1}\right)^2-1\right] + \frac{1}{4}\left|U_p^m\right| + 4\beta\tau.$$

Furthermore, we have

$$\left(1-\frac{\tau}{2}\right) + \left(\frac{1}{4}+3\beta\right)\tau\left|U_p^m\right|^2 + \left(\frac{1}{4}+\beta\right)\tau\left|U_p^{m+1}\right|^3$$
$$< \frac{3}{4} + \left(\frac{1}{4}-3\beta\right)\tau\left[\left|U_p^{m+1}\right|^3-1\right] + \frac{1}{4}\left|U_p^m\right| + 4\beta\tau,$$

namely,

$$\left(1-\frac{\tau}{2}\right) + \left(\frac{1}{4}+3\beta\right)\tau\left|U_p^m\right|^2 + 4\beta\tau\left|U_p^{m+1}\right|^3 < \frac{3}{4} - \frac{\tau}{4} + \frac{1}{4}\left|U_p^m\right| + 7\beta\tau.$$

Then we use the assumption $\left\|U^{m+1}\right\|_\infty > 1$ again to get

$$-\left(\frac{1}{4}+3\beta\right)\tau\left|U_p^m\right|^2 + \frac{1}{4}\left|U_p^m\right| + \left(\frac{1}{4}+3\beta\right)\tau - \frac{1}{4} > 0,$$

which is in contradiction with $\left|U_p^m\right| \le \|U^m\|_\infty \le 1$ provided that $\tau \le \frac{1}{2(1+12\beta)}$, so we get $\left\|U^{m+1}\right\|_\infty \le 1$. The proof of this theorem is completed. □

Next, we investigate the maximum-norm error estimate based on the discrete maximum bound principle obtained in Theorem 3.1. We omit the proof of the following theorem, since the similar result can be found in Theorem 2 in [14].

Theorem 3.2. *Assume that the exact solution $u(x,t)$ is smooth, and the initial value is smooth and bounded by 1, i.e., $\max_{x\in[a,b]}|u_0(x)| \le 1$. Assume that all the conditions in Theorem 3.1 are valid. Then, for all $1 \le n \le M$, $\|\boldsymbol{u}^n - U^n\|_\infty \le C(\varepsilon,\beta,T)(\tau^2+h^2)$, where $\boldsymbol{u}^n := (u_1^n, u_2^n, \ldots, u_N^n)^T$ represents the vector of exact solution at nth level and $C(\varepsilon,\beta,T)$ is a constant which depends on ε, β, T and the regularity of the exact solution but is independent of h and τ.*

4. The Discrete Energy Stability

In this section, we consider the discrete energy stability for scheme (2.5). Define the following discrete energy

$$E_h(U) = \frac{h}{4}\sum_{i=1}^{N}\left(U_i^2-1\right)^2 - \frac{h\varepsilon^2}{2}U^T D_h U.$$

Theorem 4.1. *The scheme (2.5) is unconditionally energy-stable, namely,*

$$E_h(U^{n+1}) \le E_h(U^n),\ n = 0, 1, \cdots, M-1.$$

Proof. Taking the difference of the discrete energy between two successive time levels, we get

$$\begin{aligned}
&E_h(U^{n+1}) - E_h(U^n)\\
=&\frac{h}{4}\sum_{i=1}^{N}\left(\left[\left(U_i^{n+1}\right)^2-1\right]^2-\left[(U_i^n)^2-1\right]^2\right)-\frac{h\varepsilon^2}{2}\left[\left(U^{n+1}\right)^T D_h U^{n+1}-(U^n)^T D_h U^n\right]\\
=&\frac{h}{4}\sum_{i=1}^{N}\left[\left(U_i^{n+1}\right)^3+(U_i^n)^3+U_i^{n+1}(U_i^n)^2+U_i^n\left(U_i^{n+1}\right)^2-2\left(U_i^{n+1}+U_i^n\right)\right]\left(U_i^{n+1}-U_i^n\right)\\
&-\frac{h\varepsilon^2}{2}\left(U^{n+1}-U^n\right)^T D_h\left(U^{n+1}+U^n\right),
\end{aligned} \tag{4.1}$$

where we used the symmetry of the matrix D_h. Taking L^2 inner product of (2.5) with $h(U^{n+1} - U^n)^T$ obtains

$$\begin{aligned}
&\frac{h}{4}\sum_{i=1}^{N}\left[\left(U_i^{n+1}\right)^3+(U_i^n)^3+U_i^{n+1}(U_i^n)^2+U_i^n\left(U_i^{n+1}\right)^2-2\left(U_i^{n+1}+U_i^n\right)\right]\left(U_i^{n+1}-U_i^n\right)\\
&+\frac{h}{\tau}\sum_{i=1}^{N}\left(U_i^{n+1}-U_i^n\right)^2+h\beta\sum_{i=1}^{N}\left(U_i^{n+1}-U_i^n\right)^4=\frac{h\varepsilon^2}{2}\left(U^{n+1}-U^n\right)^T D_h\left(U^{n+1}+U^n\right).
\end{aligned} \tag{4.2}$$

Thus, by (4.1)-(4.2), we conclude that

$$E_h(U^{n+1}) - E_h(U^n) = -\frac{h}{\tau}\sum_{i=1}^{N}\left(U_i^{n+1}-U_i^n\right)^2 - h\beta\sum_{i=1}^{N}\left(U_i^{n+1}-U_i^n\right)^4 \le 0.$$

The proof is done. □

5. Numerical Experiments

In this section, we provide three numerical examples to validate the theoretical results. The standard Newton method is used to solve the numerical scheme (2.5).

Example 1. We consider the 1D Allen-Cahn equation with the initial value

$$u_0(x) = 0.1\sin(\pi x),\ x \in (0,1).$$

For other corresponding data, we set $\varepsilon = 1/100$.

We mainly test the convergence rate for temporal discretization. Due to no analytical solution available for this numerical experiment, we define the numerical solution errors in discrete L^∞ norm as $\|U^M - U^{2M}\|_\infty$. First, fix $h = 1/500$ and choose $(\alpha,\beta) = (6/5,0), (3/2,1/12), (9/5,1/4)$. We display the errors of $\|U^M - U^{2M}\|_\infty$ with different τ in Tables 1-3, respectively. We find that the convergence orders of the errors are very close to 2. These are consistent with the convergence result obtained in Theorem 3.2.

Table 1. The errors of $\|U^M - U^{2M}\|_\infty$ with $h = 1/500$, $\alpha = 6/5$ and $\beta = 0$.

τ	$\|U^M - U^{2M}\|_\infty$ $(T=1)$	Order	$\|U^M - U^{2M}\|_\infty$ $(T=2)$	Order
$1/10$	$1.2654e-04$	$-$	$3.2620e-04$	$-$
$1/20$	$3.1598e-05$	2.0017	$8.1483e-05$	2.0012
$1/40$	$7.8973e-06$	2.0004	$2.0366e-05$	2.0003
$1/80$	$1.9742e-06$	2.0001	$5.0913e-06$	2.0000

Table 2. The errors of $\|U^M - U^{2M}\|_\infty$ with $h = 1/500$, $\alpha = 3/2$ and $\beta = 1/12$.

τ	$\|U^M - U^{2M}\|_\infty$ $(T=1)$	Order	$\|U^M - U^{2M}\|_\infty$ $(T=2)$	Order
$1/10$	$1.2597e-04$	$-$	$3.2396e-04$	$-$
$1/20$	$3.1519e-05$	1.9987	$8.1158e-05$	1.9969
$1/40$	$7.8853e-06$	1.9989	$2.0315e-05$	1.9981
$1/80$	$1.9722e-06$	1.9993	$5.0823e-06$	1.9990

Table 3. The errors of $\|U^M - U^{2M}\|_\infty$ with $h = 1/500$, $\alpha = 9/5$ and $\beta = 1/4$.

τ	$\|U^M - U^{2M}\|_\infty$ $(T=1)$	Order	$\|U^M - U^{2M}\|_\infty$ $(T=2)$	Order
$1/10$	$1.2485e-04$	$-$	$3.1958e-04$	$-$
$1/20$	$3.1368e-05$	1.9928	$8.0523e-05$	1.9886
$1/40$	$7.8635e-06$	1.9960	$2.0215e-05$	1.9939
$1/80$	$1.9687e-06$	1.9979	$5.0648e-06$	1.9968

Example 2. We consider the coarsening dynamics governed by the Allen-Cahn equation with the parameter $\varepsilon = 1/50$ and a random initial data ranging from -0.05 to 0.05. The computational domain Ω is set to be $(0,1)^2$. And the stabilized parameter β and temporal step size are chosen to be $1/4$ and $1/10$, respectively. The different fractional order $\alpha = 6/5, 3/2, 9/5$ are employed to show the validity of our scheme (2.5). As plotted in Fig. 1, it is shown that our scheme (2.5) preserves the discrete maximum bound principle and energy stability. In Fig. 2, the evolution of numerical solution is plotted for different fractional order α. It is shown that the coarsening dynamics process becomes faster when the fractional order α becomes larger, which is consistent with the existing results. This shows the effectiveness of our scheme.

Exmaple 3. We consider the different shrinking bubble problem governed by the Allen-Cahn equation. The stabilized parameter β and temporal step size are the same as in Example 2. Then we consider the standard shrinking bubble problem with fractional order $\alpha = 9/5$, parameter $\varepsilon = 1/30$ and $\Omega = (-1,1)^2$. The star shape shrinking bubble problem with $\alpha = 9/5$, parameter $\varepsilon = 1/50$ and $\Omega = (0,1)^2$. The spatial step sizes are set to $1/50$ and $1/100$. The initial condition of standard bubble is a sphere of Radius 0.2 located original point,

$$u_0(x) = \begin{cases} 1, & |x|^2 < 0.2^2, \\ -1, & |x|^2 \geq 0.2^2. \end{cases}$$

The star shape is given by

$$u_0(x,y) = \tanh\left(\frac{0.25 + \cos(6\theta) - \sqrt{(x-0.5)^2 + (y-0.5)^2}}{\sqrt{2}\varepsilon}\right),$$

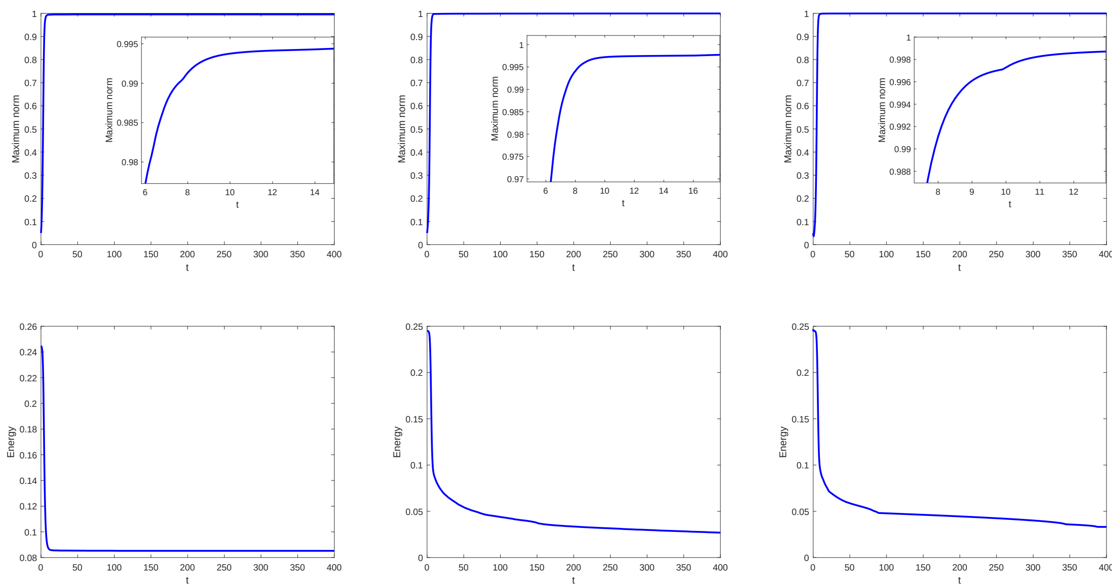

FIGURE 1. The evolutions of maximum norm (top) and energy (bottom) with $\alpha = 6/5, 3/2, 9/5$ (from left to right).

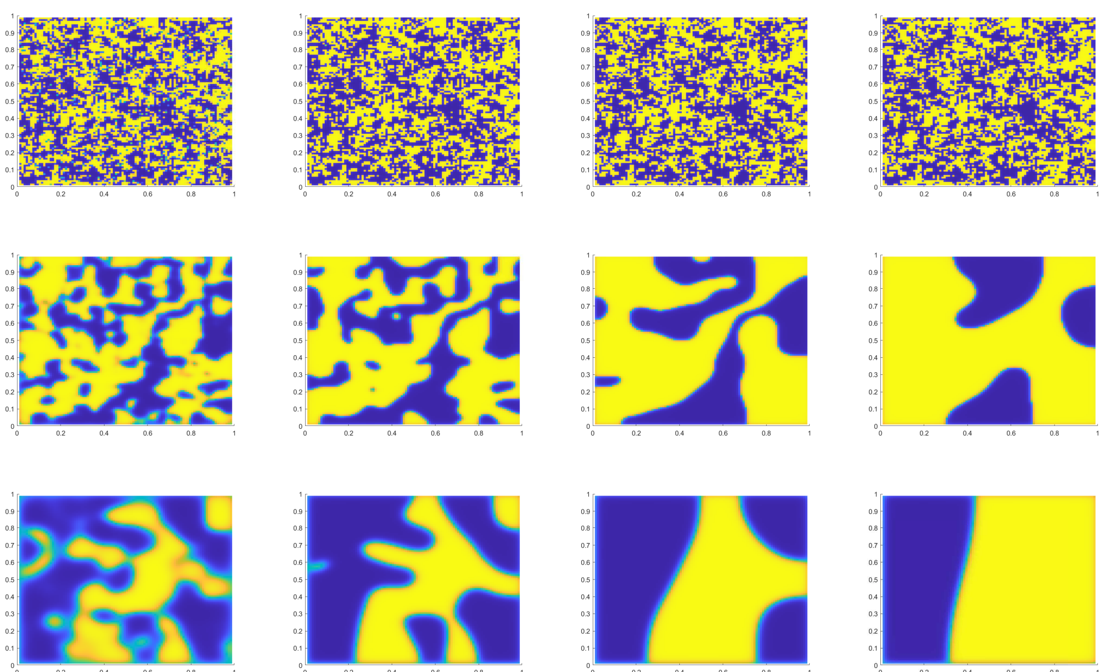

FIGURE 2. The evolutions of numerical solution at $t = 8, 20, 100, 400$ (from left to right) with different fractional order $\alpha = 6/5, 3/2, 9/5$ (from top to bottom).

where

$$\theta = \begin{cases} \arctan\left(\dfrac{y-0.5}{x-0.5}\right), & x > 0.5, \\ \pi + \arctan\left(\dfrac{y-0.5}{x-0.5}\right), & \text{otherwise}. \end{cases}$$

Several snapshots are presented to display the time evolutions of phase structure at different time for standard and star shape bubble shrinking problems in Fig. 3 and Fig. 4.

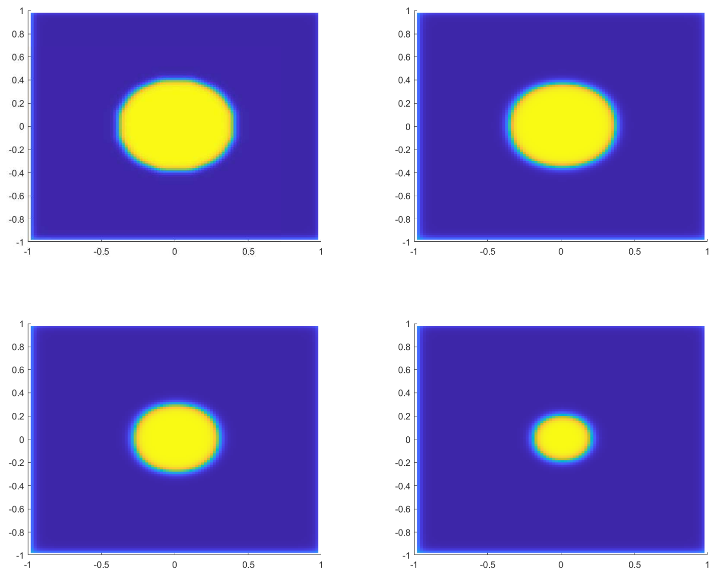

FIGURE 3. Snapshots of standard bubble shrinking problem at time $t = 1, 20, 60, 100$ (from top to bottom and left to right).

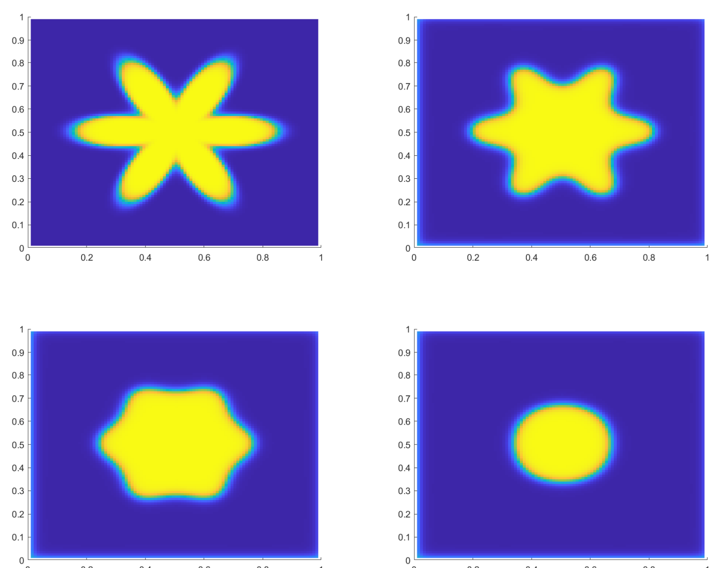

FIGURE 4. Snapshots of star shape bubble shrinking problem at time $t = 0, 8, 20, 100$ (from top to bottom and left to right).

Acknowledgments

This work was supported by the National Natural Science Foundation of China (Grant No. 12426629).

REFERENCES

[1] S. M. Allen, J. W. Cahn, A microscopic theory for antiphase boundary motion and its application to antiphase domain coarsening, Acta Metall. 27 (1979), 1085-1095.

[2] Q. Du, L. Ju, X. Li, et al, Maximum principle preserving exponential time differencing schemes for the nonlocal Allen-Cahn equation, SIAM J. Numer. Anal. 57(2) (2019), 875-898.

[3] C. Çelik, M. Duman, Crank-Nicolson method for the fractional diffusion equation with the Riesz fractional derivative, J. Comput. Phy. 231(4) (2012), 1743-1750.

[4] T. Hou, T. Tang, J. Yang, Numerical analysis of fully discretized Crank-Nicolson scheme for fractional-in-space Allen-Cahn equations, J. Sci. Comput. 72(3) (2017), 1214-1231.

[5] T. Hou, D. Xiu, W. Jiang, A new second-order maximum-principle preserving finite difference scheme for Allen-Cahn equations with periodic boundary conditions, Appl. Math. Lett. 104 (2020), 106265.

[6] L. Ju, X. Li, Z. Qiao, Generalized SAV-exponential integrator schemes for Allen-Cahn type gradient flows, SIAM J. Numer. Anal. 60(4) (2022), 1905-1931.

[7] H. Liao, T. Tang, T. Zhou, A second-order and nonuniform time-stepping maximum-principle preserving scheme for time-fractional Allen-Cahn equations, J. Comput. Phy. 414 (2020), 109473.

[8] H. Liao, T. Tang, T. Zhou, An energy stable and maximum bound preserving scheme with variable time steps for time fractional Allen-Cahn equation, SIAM J. Sci. Comput. 43(5) (2021), A3503-A3526.

[9] B. Li, J. Yang, Z. Zhou, Arbitrarily high-order exponential cut-off methods for preserving maximum principle of parabolic equations, SIAM J. Sci. Comput. 42(6) (2020), A3957-A3978.

[10] J. Shen, T. Tang, J. Yang, On the maximum principle preserving schemes for the generlized Allen-Cahn equation, Commu. Math. Sci. 14(6) (2016), 1517-1534.

[11] T. Tang, J. Yang, Implicit-explicit scheme for the Allen-Cahn equation preserves the maximum principle, J. Comput. Math. 34 (2016), 471-481.

[12] Z. Weng, S. Zhai, W. Dai, Y. Yang, Y. Mo, Stability and error estimates of Strang splitting method for the nonlocal ternary conservative Allen-Cahn model, J. Comput. Appl. Math. 441 (2024), 115668.

[13] Z. Xu, Y. Fu, Unconditional energy stability and maximum principle preserving scheme for the Allen-Cahn equation, Numer. Algo. 99 (2025), 355-376.

[14] C. Xu, Y. Cao, T. Hou, Numerical analysis of a second-order finite difference scheme for Riesz space-fractional Allen-Cahn equations, Adv. Cont. Discr. Mod. 2025 (2025), 2.

[15] S. Zhai, Z. Weng, Y. Mo, X. Feng, Energy dissipation and maximum bound principle preserving scheme for solving a nonlocal ternary Allen-Cahn model, Comput. Math. Appl. 155 (2024), 150-164.

[16] H. Zhang, J. Yan, X. Qian, X. Gu, S. Song, On the preserving of the maximum principle and energy stability of high-order implicit-explicit Runge-Kutta schemes for the space-fractional Allen-Cahn equation, Numer. Algo. 88 (2021), 1309-1336.